frontiers in Mechanical Engineering

ORIGINAL RESEARCH
published: 20 June 2019
doi: 10.3389/fmech.2019.00034

An Experimental Study of Intermittent Heating Frequencies From Wind-Driven Flames

Wei Tang[1]*, *Mark Finney*[2], *Sara McAllister*[2] and *Michael Gollner*[1]*

[1] Department of Fire Protection Engineering, University of Maryland, College Park, MD, United States, [2] United States Forest Service (USDA), Missoula Fire Sciences Laboratory, Missoula, MT, United States

An experimental study was conducted to understand the intermittent heating behavior downstream of a gaseous line burner under forced flow conditions. While previous studies have addressed time-averaged properties, here measurements of the flame location and intermittent heat flux profile help to give a time-dependent picture of downstream heating from the flame, useful for understanding wind-driven flame spread. Two frequencies are extracted from experiments, the maximum flame forward pulsation frequency in the direction of the wind, which helps describe the motion of the flame, and the local flame-fuel contact frequency in the flame region, which is useful in calculating the actual heat flux that can be received by the unburnt fuel via direct flame contact. The forward pulsation frequency is obtained through video analysis using a variable interval time average (VITA) method. Scaling analysis indicates that the flame forward pulsation frequency varies as a power-law function of the Froude number and fire heat-release rate, $f_F \tilde{} \left(Fr/Q^{*1/2}\right)^{0.4}$. For the local flame-fuel contact frequency, it is found that the non-dimensional flame-fuel contact frequency f_C^+ remains approximately constant before the local Ri_x reaches 1, e.g., attached flames. When $Ri_x > 1$, f_C^+ decreases with local as Ri_x flames lift up. A piece-wise function was proposed to predict the local flame-fuel contact frequency including the two Ri_x scenarios. Information from this study helps to shed light on the intermittent behavior of flames under wind, which may be a critical factor in explaining the mechanisms of forward flame spread in wildland and other similar wind-driven fires.

Keywords: wind-driven, wildfire, flame spread, pulsation frequency, flame contact

OPEN ACCESS

Edited by:
Guillermo Rein, Imperial College London, United Kingdom

Reviewed by:
Longhua Hu, University of Science and Technology of China, China
Khanh Duc Cung, Southwest Research Institute, United States

***Correspondence:**
Wei Tang
wtang125@gmail.com
Michael Gollner
mgollner@umd.edu

Specialty section:
This article was submitted to Thermal and Mass Transport, a section of the journal Frontiers in Mechanical Engineering

Received: *28 February 2019*
Accepted: *28 May 2019*
Published: *20 June 2019*

Citation:
Tang W, Finney M, McAllister S and Gollner M (2019) An Experimental Study of Intermittent Heating Frequencies From Wind-Driven Flames. Front. Mech. Eng. 5:34. doi: 10.3389/fmech.2019.00034

INTRODUCTION

Wind-driven fires have been studied extensively over the past few decades, however, there are still significant gaps in understanding, especially applied to wind-driven fires resembling a line fire configuration. Most of the current literature on wind-driven fire spread has focused on the steady-state burning characteristics of these fires, preferring this time-averaged view of flame tilt angles, burning rates and downstream heat fluxes to the more complicated, stochastic movements that flames in reality make (Putnam, 1965; Albini, 1982; Weckman and Sobiesiak, 1988). The fluctuation of the flame front has recently been determined to follow some scaling laws and play a role in flame spread, in particular for wildland fires (Finney et al., 2015). The movement of flames therefore may have implications in a variety of wind-driven scenarios, wherever flames reside long enough to heat unburnt fuels and thus contribute to forward fire spread.

Flame "pulsations," or brief cyclical motions, have been studied for various fire configurations. Under stagnant conditions, an intermittent "puffing" phenomenon has been extensively studied using pool fires where the puffing frequency of the flame has been found to be well correlated with the diameter of the fire source (Grant and Jones, 1975; Hamins et al., 1992; Hu et al., 2015). These experiments on buoyant plumes suggest that puffing is primarily the result of a buoyant flow instability, which involves the strong coupled interaction of a toroidal vortex formed a short distance above a fuel or burner surface (Cetegen and Ahmed, 1993). Scaling of this phenomena has also been represented as a Strouhal–Froude relationship $St \sim Fr^{-0.5}$ (Cetegen and Ahmed, 1993). In wind-driven fires, the pulsation of the flame is not expected to scale with burner size in the same way as fires under stagnant conditions as wind plays a significant role in the fire behavior, too. These fires have already been shown to be strongly influenced by a competition between upward buoyant forces from the flame and forward momentum from the wind (Tang et al., 2017a), suggesting a combination of these forces will also play a role in generating intermittent motions within the flame.

A detailed look at the time-dependent nature of wind-blown flames reveals that there are a variety of structures and regions which vary in both time-dependent and averaged characteristics. **Figure 1** shows an image of a wind-blown flame from a stationary burner that, at first, appears attached along the downstream surface, but eventually lifts into a tilted flame. Three regions are thus defined to describe the flame behavior. First, an attachment region exists where the flame is visibly attached to the surface, occurring for some distance downstream of the burner since the wind overpowers buoyancy from the flame. As the flame moves forward, buoyancy increases in proportion to the momentum from the wind and the flame enters a transitional, "intermittent" region, where the flame fluctuates as a result of the competition with momentum from the wind and flame-generated buoyancy. After this region, the flame is finally lifted due to the dominant role of buoyancy, growing with distance as distributed heat release reactions continues to occur within the flame.

In the process of the flame moving forward, a two-directional fluctuating behavior is anticipated, indicated on **Figure 1**. One is *flame forward pulsation*, where the flame intermittently flickers forward onto the downstream surface ahead of the flame front. In a spreading fire scenario, this may potentially reach more unburnt fuels and heat them, albeit for short times. This likely occurs due to a competition between momentum-driven wind and a counter-clockwise recirculation zone at the flame front, a buoyant instability similar to puffing pool fires, or a combination of the two. The other is *flame-fuel contact*, which appears most rapid in the region between the attached flame length and the lifted region. The up-and-down motion of the flame here is most likely due to a local buoyant instability and may be subject to change along the downstream distance. Independently measuring these two components will help to determine the influence intermittent heating has in each of the mentioned regions. Flame *forward pulsation* and *flame-fuel contact* will each play a significant role in the ignition of unburnt fuels within the flame's reach in wind-driven fires.

In our previous work (Tang et al., 2017a), the local total heat flux distribution on the downstream surface of wind-driven line fires was investigated and a local Richardson number [$Ri_x = Gr_x/Re_x^2$, describing flame buoyancy over wind momentum (Subbarao and Cantwell, 1992; Johnson and Kostiuk, 2000)] was employed to scale measured non-dimensional heat fluxes. Inertial forces would be expected to dominate the flame behavior when $Ri_x < 0.1$, and buoyant forces when $Ri_x > 10$. However, the details and implications of the heat transfer modes in the mixed region ($0.1 < Ri_x < 10$), where the transition from an inertial-dominant to buoyancy-dominant regime, has not been well studied. Because most fires with cross-flow reside in this region, e.g., flames that begin attached near the surface and tend to "lift off" into a more plume-like scenario downstream, study of the fire behavior in this region is important to improve understanding of heating during flame spread.

In this study, a stationary, non-spreading gas-burner fire configuration was chosen as it allows for a thorough statistical analysis of the flame structure. Long-duration experiments allow for a large sample size and more control over variations in experimental parameters, such as decoupling the heat-release rate of the fire from flow conditions. High speed video is useful on these fires to reveal and track buoyant instabilities in the fire flow which resemble those appearing in spatially-uniform fuel beds. The same flame movements observed in previous spreading fire experiments were observed with the stationary burner (Finney et al., 2015), but with the ability to collect a larger data set of intermittency. Both forward and vertical movements of the flame were studied. The flame forward pulsation frequency was extracted from videos using the VITA method, similar to previous work (Tang et al., 2017b), while the local flame-fuel contact frequency on the downstream surface was obtained through Fast Fourier Transform (FFT) of heat flux sensor data. Scaling laws were then developed for these two frequencies and equations derived to correlate the frequency with related controlling parameters.

EXPERIMENTAL SETUP

Experiments were performed on a specially-designed 30 cm cross-section laminar blower built for uniform forced-flow combustion experiments. The blower pressurizes a 0.75 cubic-meter plenum with a centrifugal fan. The flow then travels through a converging section into a 30 × 30 cm rectangular duct, where multiple mesh screens and honeycomb flow straighteners were installed in the converging section to help generate a uniform wind profile. Finally, the flow travels another 1.35 m in the duct resulting in a fully-developed laminar boundary layer before it is exhausted at the outlet. The outlet velocity from the tunnel can be as high as 6 m/s, with a turbulence intensity, u'/u controlled below 3%. The wind velocity ranged from about 0.8 to 2.5 m/s in experiments, confirmed to be

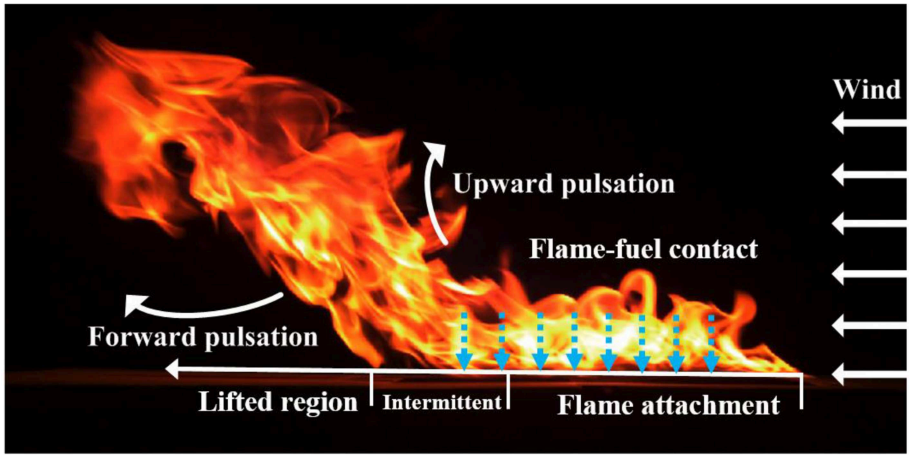

FIGURE 1 | The movement of a stationary, wind-driven flame is depicted here with forward and upward pulsations and flame-fuel contact depicted throughout the attached, intermittent and lifted regions of the flame.

uniform at multiple locations across the space with a hot-wire anemometer.

The experimental platform was placed immediately following the outlet of the exhaust tunnel. A sand-filled gas burner was used with a 10 cm deep sand-filled plenum and a 25 cm (length) ×5 cm (width) surface. The top surface of the burner was mounted flush with a sheet of ceramic insulation board in the center of the blower outlet. The ceramic board had dimensions of 90 (length) × 45 (width) × 2 (height) cm^3, over which the flame fluctuates, providing a quasi-adiabatic boundary condition. Propane from a gas cylinder was passed through a programmable flow meter to provide a steady flow rate of fuel during experiments. Three different fire heat-release rates, 6.3, 7.9, 9.5 kW, which correspond to 4, 5, and 6 liters per minute of propane gas were used during the experiments. High-speed videography using a Nikon DX was recorded at 250 frames per second at a 1,000 × 720 pixel resolution to capture digital images of the flame in all configurations from the side view. The wind tunnel and test section setup are shown in **Figures 2A,B**.

For the frequency of the flame intermittently attaching to the downstream surface, a Gardon-type high frequency Vatell heat flux gauge (model HFM 1000-0) sampled at 1 kHz was used to capture the heat flux signal, and a FFT is applied to the heat flux data to extract the dominant frequency. These gauges were placed at six downstream locations 5.5 cm apart, starting 5.5 cm away from the trailing edge of the burner. Experimental conditions were chosen following our previous work on the total heat flux distribution and flame attachment, representing a wide range of wind momentum (Re number) and flame buoyancy (non-dimensional heat release rate) (Tang et al., 2017a). For the flame-forward pulsation frequency, a dominant frequency is not as apparent in the video analysis, as it is thought to be more affected by transport of stochastic turbulent structures. A technique used to analyze such turbulent flows, the variable-interval time-average (VITA) method, essentially a level-crossing technique, is applied through a MATLAB script which was previously found to show good results for turbulent flows (Tang et al., 2017b).

RESULTS AND DISCUSSIONS

Flame Forward Pulsation Frequency

The flame forward pulsation was measured for stationary burners under wind. The flame location was determined using side-view high speed videos. Each image in the video was cropped to the same region-of-interest, a region defined from the downstream edge of the burner surface to the end of the image in the downstream direction, with a certain height above the surface. This region, in theory, could represent a flame zone depth in a spreading fire (see the dashed rectangle in **Figure 3A**). Flame images were then converted to greyscale images in MATLAB by averaging all three color channels and a threshold applied to result in a black-and-white image of flame and no-flame regions. As shown in **Figure 3A**, the flame position and flame shape are constantly changing when there is a perpendicular wind. The flame location is determined in the region of interest by tracking the furthest downstream tip of the flame detected from thresholding. This location fluctuates in time and would "burst" or quickly enter into what would be the unburnt fuel region, resulting in the intermittent heating of unburnt fuels by flame contact.

Resultant flame locations as a function of time were analyzed using the VITA method (Blackwelder and Kaplan, 1976; Audouin et al., 1995) for a 1 cm window in the video at different distances downstream of the burner. Other window sizes up to 4 cm wide required more processing but produced similar results. Level-crossing was only considered for the forward direction, thus only when the flame appeared after absence in the previous frame, was it considered a crossing to avoid double-counting. The resulting flame forward pulsation frequency was then determined at each downstream location by dividing the number of crossings by the total number of frames,

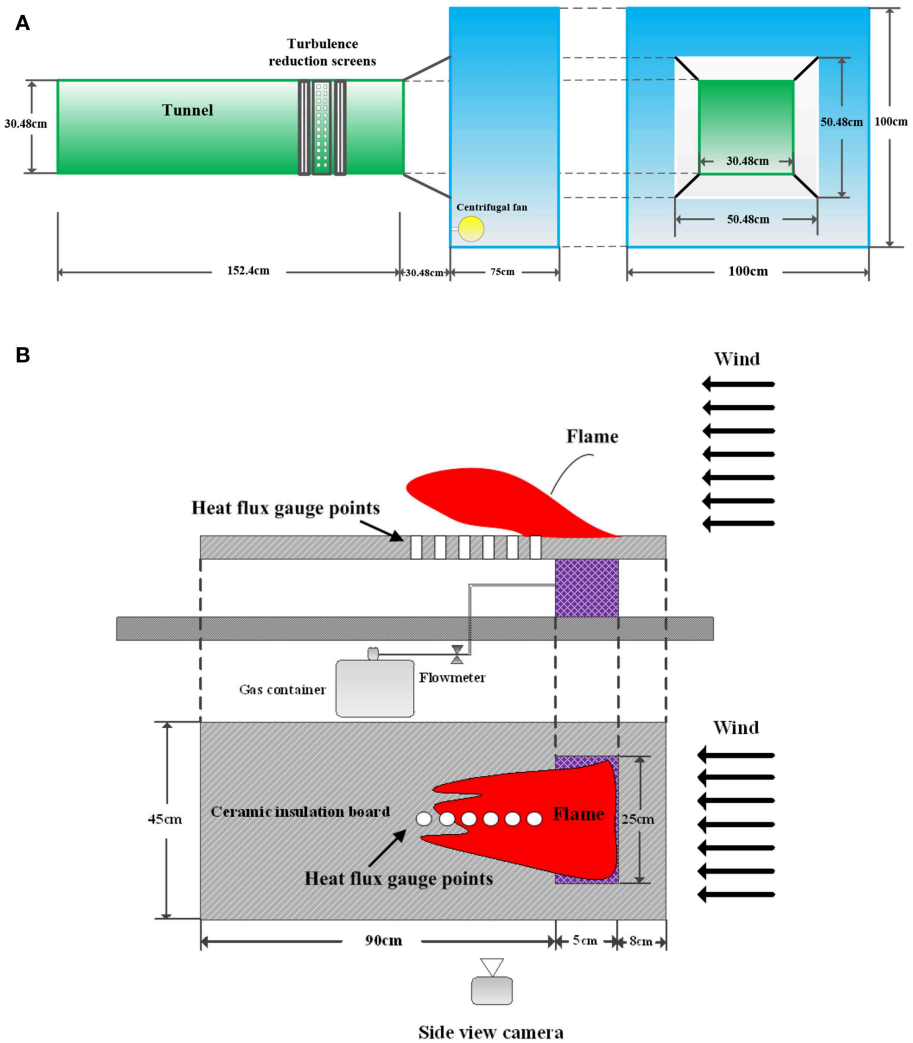

FIGURE 2 | Experimental setup. **(A)** Wind tunnel apparatus. **(B)** Test section setup.

multiplied by the frame rate of the video. The mean values of the frequency data obtained from all the thresholds was used for later analysis. To connect results to flame spread in solid fuels, a fuel bed height will need to be defined for the scenario at hand. **Figure 3B** shows resultant frequencies following application of the VITA technique. As the flame intermittently moves forward and backwards, it enters and leaves the downstream window position producing a parabolic distribution of frequencies. A maximum frequency therefore occurs at some downstream location between the continuous flame region and the maximum forward extension of the flame. The frequency at this location is used in the analysis as a maximum representative frequency of the flame along the surface.

Applying the VITA method to all fire sizes and wind velocities, maximum frequencies are extracted, shown in **Figure 4**. It shows that the flame pulsation frequency increases relatively linearly with the wind velocity, while it decreases with fire size in all the experiments tested. The frequencies observed range from <10 Hz to about 15 Hz.

Flame-Fuel Contact Frequency

The flame-fuel contact frequency can help determine how much heat flux is received by unburnt fuels ahead of the flame front through direct flame contact, which has recently been found to be a primary mechanism of ignition of fuels in a wind-driven wildland fire (Finney et al., 2015). For each of the experimental conditions, raw heat flux signals were taken at different locations on the downstream board. The flame-fuel contact frequency was extracted from measured heat flux signals by applying a FFT which results in a frequency spectrum.

The same method was applied to three cases with different wind velocities but the same fire size (9.5 kW) at 11 cm downstream, shown in **Figure 5**. FFT data smoothed by a Savitzky–Golay filter revealed the peak intensity used to choose the peak frequency at that location. In **Figure 5**, it can be seen

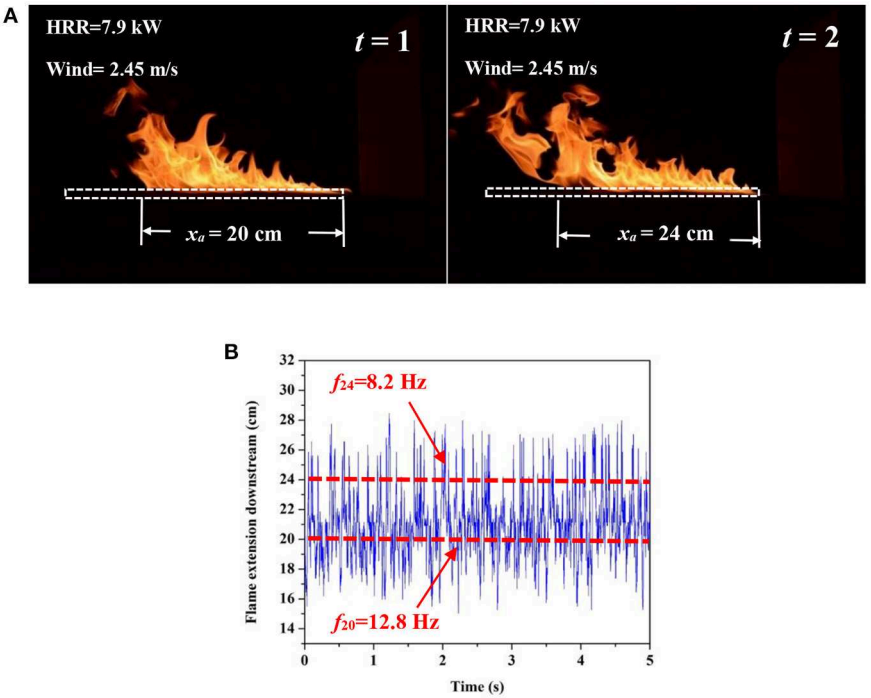

FIGURE 3 | Flame location between two time steps in a forced flow experiment and resultant flame locations with time. **(A)** Flame image in two consecutive time steps. **(B)** Flame extension distance downstream.

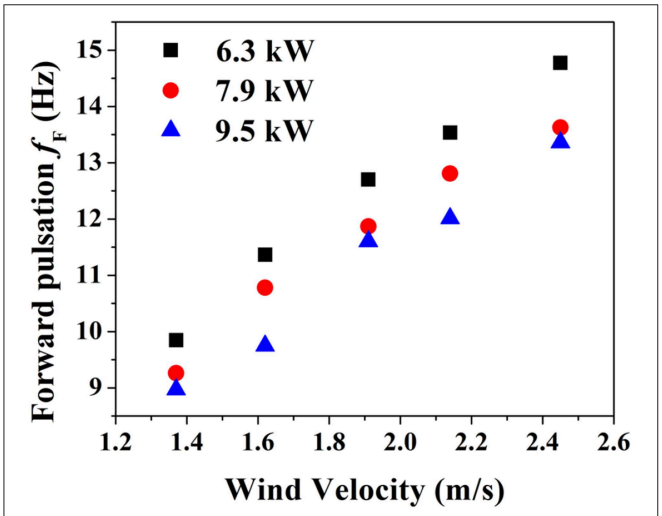

FIGURE 4 | Forward pulsation frequencies with different wind velocities and fire sizes.

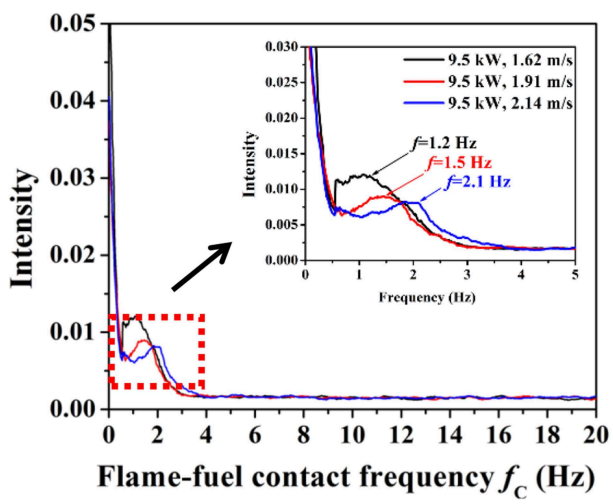

FIGURE 5 | Comparison of frequencies obtained from a FFT for different wind velocities.

that the flame-fuel contact frequency slightly increases with increasing wind velocity, however the intensity of this peak decreases indicating a reduced dominance of this peak frequency and more turbulent structures.

The local flame-fuel contact frequency was further plotted for different wind velocity and fire sizes. **Figure 6** shows one example where the fire size is 7.9 kW, for a given wind velocity, the local frequency tends to decrease with downstream distance from the burner. It is worth noting that, under high wind speeds, the flame starts to behave differently as the leading edge of the flame becomes highly strained i.e., the flame length approaches a constant value instead of extending further with high wind

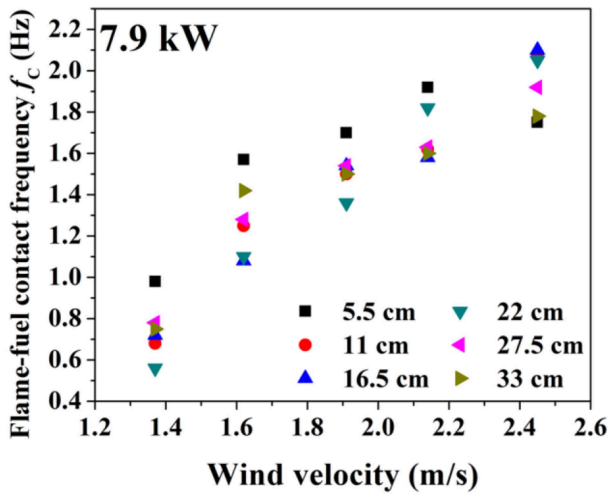

FIGURE 6 | Local flame fuel contact frequency for a 7.9 kW fire under different wind velocities.

speed, the leading edge also starts to briefly extinguish and blue flames appear, which might explain some of the decrease shown in **Figure 6** for the high wind at 5.5 cm data point.

Discussion

Unlike previous studies on flame frequencies (Hamins et al., 1992; Cetegen and Ahmed, 1993), which focused on puffing under stagnant conditions, this paper investigated the flame pulsation frequency under a cross-wind flow. The puffing frequency without wind has been found to be a function of burner size. Under wind conditions, however, two movements have been clearly identified. One is the global forward pulsation, where the flame is driven by the wind, and possibly buoyancy as well, and intermittently moves back and forth in the stream-wise direction. The other is an upward pulsation, which is found to be a more local phenomenon, where the flame is touching and directly transferring heat to the local unburnt fuel within the attachment and intermittent regions shown in **Figure 1**. This section will discuss these two pulsation frequencies and their correlations with relevant parameters.

Global Flame Forward Pulsation Frequency

The global flame forward pulsation frequency is thought to be the result of a competition between forward momentum from the ambient wind and buoyancy from the flame itself. A scaling analysis can be performed, assuming relevant parameters, which reveals two primary groups that the forward pulsation frequency is dependent on, the Froude number (wind momentum over inertial force) and Q* (buoyancy). A phenomenological explanation can be arrived at by first assuming the flame forward-pulsation frequency can be related to both the ambient wind velocity, u and the flame length, l_f, which characterizes buoyancy from the fire, as

$$f_F \tilde{} \frac{u}{l_f}. \tag{1}$$

In a wind-driven fire, the flame length has previously been found to be a function of the wind velocity and mass burning rate in the form (Thomas, 1963; Moorhouse, 1982),

$$\frac{l_f}{D} = a\left(\frac{\dot{m}''}{\rho_a\sqrt{gD}}\right)^b \cdot (u^*)^c, \tag{2}$$

where D is the characteristic diameter or length of the burner, $\dot{m}''$ the mass burning rate of the fire, and a, b, and c are constants, previously found to be 62, 0.25, −0.044, respectively for gas fires (Thomas, 1963). A non-dimensional velocity can be defined as a ratio of the ambient wind velocity and a characteristic buoyant velocity of the fire (Hu, 2017),

$$u^* = \frac{u}{\left(g\dot{m}''D/\rho_a\right)^{1/3}}, \tag{3}$$

where g is the acceleration due to gravity and ρ_a the density of ambient air. Assuming the fuel burns completely, $\dot{m}''$can be related to the heat-release rate of the fire, $\dot{Q}$ as

$$\dot{Q} = \Delta H_c \dot{m}'', \tag{4}$$

which provides a more functional and universal parameter from which to define the fire. The heat-release rate can be non-dimensionalized as Q^* (Quintiere, 1989) for a fire plume and expressed in terms of $\dot{m}''$ as

$$Q^* = \frac{\dot{Q}}{\rho_a T_a C_p \sqrt{gD^5}} \tilde{} \dot{m}'', \tag{5}$$

Combining Equations (1–5), we arrive at Equation (6), which relates the flame forward-pulsation frequency with the Froude number and the non-dimensional heat-release rate,

$$f_F \sim \frac{u^{1.044}}{Q^{*0.265}} \approx \frac{\mathrm{Fr}^{1/2}}{Q^{*1/4}} = \sqrt{\frac{\mathrm{Fr}}{Q^{*1/2}}}, \tag{6}$$

where Fr is defined as $\mathrm{Fr} = u^2/gL$, u is the wind velocity, and L is the flame length. The flame forward pulsation frequency is then plotted against this parameter derived in **Figure 7**, and a power-law relationship is found relating them. An empirical fit can then be found from the data,

$$f_F = 15.7\left(\frac{\mathrm{Fr}^{1/2}}{Q^{*1/4}}\right)^{0.8} = 15.7\left(\frac{\mathrm{Fr}}{Q^{*1/2}}\right)^{0.4}. \tag{7}$$

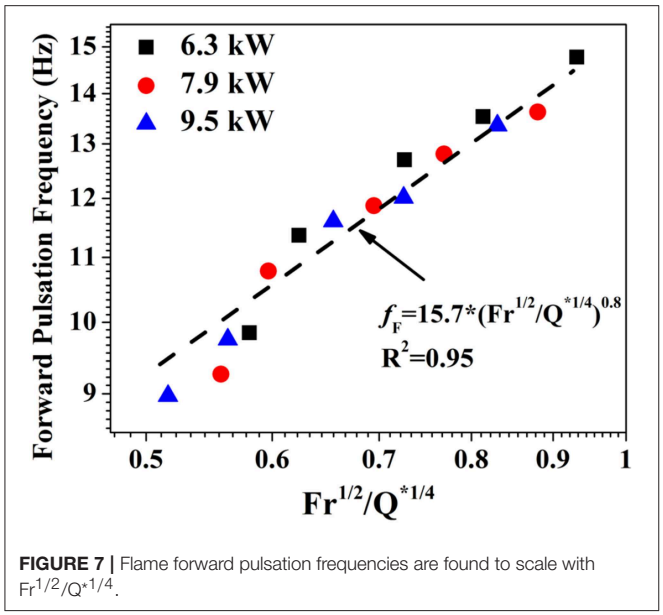

FIGURE 7 | Flame forward pulsation frequencies are found to scale with $Fr^{1/2}/Q^{*1/4}$.

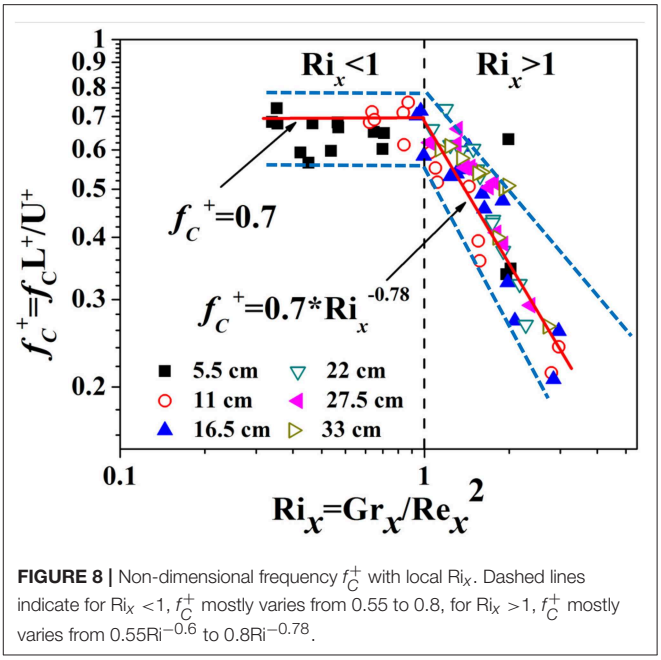

FIGURE 8 | Non-dimensional frequency f_C^+ with local Ri_x. Dashed lines indicate for Ri_x <1, f_C^+ mostly varies from 0.55 to 0.8, for Ri_x >1, f_C^+ mostly varies from $0.55Ri^{-0.6}$ to $0.8Ri^{-0.78}$.

with an R^2 of 0.95. While f_F could be presented in non-dimensional form, such as through a Strouhal number, the choice of a relevant length scale known *a priori* is difficult to define and, if properly applied, will result in a straight line similar to puffing pool fires (Hamins et al., 1992). Therefore, only f_F is shown in **Figure 7**.

Local Flame-Fuel Contact Frequency

For the local flame-fuel contact frequency, the local Grashof ($Gr_x = g\beta(T_h - T_\infty)L^3/\nu^2$) and Reynolds ($Re_x = UL/\nu$) numbers arise as critical parameters describing the flow and heat transfer in our setup, where T_h and $T_\infty$are the hot gas and ambient temperatures, respectively, L is the characteristic length, g the acceleration due to gravity, β the thermal expansion coefficient, and ν the kinematic viscosity of the ambient air. The relative role of buoyant and inertial forces in the flow have been found to be well-described by comparing the relative influence of these two parameters, often determined to be Gr_x/Re_x^a, with a varying constant a (Imura et al., 1978; Miller et al., 2017).

A non-dimensional flame-fuel contact frequency f_C^+ is proposed based on a characteristic gas fuel flow rate and downstream distance,

$$f_C{}^+ = \frac{f_C L^+}{u^+}, \tag{8}$$

$$u^+ = \left(g\dot{m}'' D/\rho_a\right)^{1/3}. \tag{9}$$

where $f_C$is the raw frequency data we obtained from heat flux gauge sensor, L^+ is the downstream distance from the measuring point to the leading edge of the burner chosen as characteristic length scale, u^+ is the characteristic fuel velocity based on mass flow rate, $\dot{m}''$ is the mass flow rate, D the burner hydraulic diameter, and ρ_a the air density.

Note that this non-dimensional flame-fuel contact frequency is not a typical form of the Strouhal number, such as those previously defined in pool fire studies. St-Fr correlations have been found to correlate the pool fire puffing frequency under stagnant conditions, where only natural convection is controlling the flame behavior, and the length scale chosen for the study was the pool diameter. This appears to be more of a global instability of the system driven by buoyancy. In our study, we introduce forced convection (wind), and the length scale is chosen as the distance from the measuring point to the leading edge of the burner, where the thermal boundary layer starts to develop. The length scale chosen in this paper follows our previous work on the effect of forced and natural convection on the heat flux distribution in wind-driven line fires (Tang et al., 2017a).

In **Figure 8** the local Ri_x is plotted against the non-dimensional frequency. When Ri_x is smaller than 1, f_C^+ varies around 0.7 with ranges from 0.55 to 0.8, however after Ri_x reaches 1, f_C^+ starts to decrease with Ri_x. A piece-wise function was obtained based on a correlation with experimental data to describe the local frequency trend with Ri_x. Equation (10) indicates that in a wind-driven fire, the flame-fuel contact frequency before the local Ri_x reaches 1 will remain unchanged, fluctuating around $f_C^+ = 0.7$. After Ri_x reaches 1, which means natural convection and forced convection approximately balance each other, f_C^+ will decrease with Ri_x in a power law trend as $f_C^+ = 0.7Ri_x^{-0.78}$. Correlations are provided here is to aid in understanding the trend of local flame-fuel contact frequency as it changes in different Ri_x regimes. Within the two Ri_x regimes representing lifted and attached flames, data are still scattered to some degree. Further investigations are needed to look into each of these regimes and isolate the parameters related to this scatter, which may include the fuel heat-release rate, geometry of the burner, etc., to obtain a full understanding of this relationship.

$$f_C{}^{+} = \begin{cases} 0.7 & Ri_x < 1 \\ 0.7\mathrm{Ri}_x^{-0.78} & Ri_x > 1 \end{cases} \quad (10)$$

This investigation revealed multiple patterns of movement within a wind-driven flame resulting from different forces controlling the competition between buoyancy and forward momentum along the length of the flame. Neither puffing pool fires nor jets in cross flow correctly describe this phenomenon.

The forward motion is more "messy" than the up and down contact of the flame. This likely occurs due to a competition between momentum-driven wind and a counter-clockwise recirculation zone at the flame front, a buoyant instability similar to puffing pool fires, or a combination of the two. It is also thought to be more affected by transport of stochastic turbulent structures. The up and down motion of the flame, described by $f_C^+$and $\mathrm{Ri_x}$ is seen in two regions, similar to previous studies investigating the heat flux downstream of the burner. The changes here were attributed to attachment and liftoff of the flame, which appears to be occurring here as well. It is near the end of this attachment region where the highest frequencies are observed, indicating this is also an inflection point where an unstable transition between attachment and liftoff occurs.

The way in which the flame moves within both the forward region ahead of and close within the attachment region may have important implications for fire spread modeling. Current flame spread models assume either a constant heat flux for some distance ahead of the burning region, which heats unignited fuels, or a profile of decaying heat flux constant with time. Both approaches neglect the time-dependence of heating that becomes increasingly important when fine fuels primarily carry the fire, such as in wildland fires.

CONCLUSIONS

Experiments were conducted on a variety wind-driven line fires where the intermittent behavior of the flame was studied. Both the flame forward-pulsation frequency and flame-fuel contact frequency were independently measured. Trends in these quantities were reviewed and non-dimensional scaling proposed for each. It was found that the flame forward pulsation frequencyf_F, can be well correlated and predicted by a non-dimensional parameter, $^{\mathrm{Fr}}/_{Q^{*1/2}}$ in a power law trend. The mechanism for this forward pulsation has been found to be related to the competition of wind momentum and flame buoyancy. For the flame-fuel contact frequency, which describes the local heating process of the flame to unburnt fuels along the flame attachment and intermittent regions, a piece-wise function was found with local Ri_x, indicating that when $\mathrm{Ri}_x < 1$, the non-dimensional flame contact frequency f_C^+ remains approximately constant, and when $\mathrm{Ri}_x > 1$, it decreases with Ri_x. The description of global flame forward pulsation frequency and local flame-fuel contact frequency will help to explain wildland fuel ignition and flame spread in the future.

DATA AVAILABILITY

All datasets generated for this study are included in the manuscript and/or the supplementary files.

AUTHOR CONTRIBUTIONS

WT and MG designed the tests and conducted the tests. WT, MF, MG, and SM wrote the paper.

ACKNOWLEDGMENTS

The authors would like to acknowledge financial support for this work from the USDA Forest Service Missoula Fire Sciences Laboratory and National Fire Decision Support Center under collaborative agreement 13-CS-11221637-124 and CBET 1554026. The authors also would like to thank Dr. Arnaud Trouve, Dr. Colin Miller, Mr. Daniel Gorham for their fruitful discussions and insightful comments.

REFERENCES

Albini, F. A. (1982). Response of free-burning fires to nonsteady wind. *Combust. Science Tech*. 29, 225–241. doi: 10.1080/00102208208923599

Audouin, L., Kolb, G., Torero, J. L., and Most, J. M. (1995). Average centreline temperatures of a buoyant pool fire obtained by image processing of video recordings. *Fire Safety J*. 24, 167–187. doi: 10.1016/0379-7112(95)00021-K

Blackwelder, R. F., and Kaplan, R. E. (1976). On the wall structure of the turbulent boundary layer. *J. Fluid Mech*. 76, 89–112. doi: 10.1017/S0022112076003145

Cetegen, B. M., and Ahmed, T. (1993). Experiments on the periodic instability of buoyant plumes and pool fires. *Combust. Flame* 93, 157–184. doi: 10.1016/0010-2180(93)90090-P

Finney, M., Cohen, J., Forthofer, J., McAllister, S., Gollner, M., Gorham, D., et al. (2015). Role of buoyant flame dynamics in wildfire spread. *Proc. Natl. Acad. Sci. U.S.A*. 112, 9833–9838. doi: 10.1073/pnas.1504498112

Grant, A. J., and Jones, J. M. (1975). Low-frequency diffusion flame oscillations. *Combust. Flame* 25, 153–160. doi: 10.1016/0010-2180(75)90081-4

Hamins, A., Yang, J. C., and Kashiwagi, T. (1992). An experimental investigation of the pulsation frequency of flames. *Proc. Combust. Inst*. 24, 1695–1702. doi: 10.1016/S0082-0784(06)80198-0

Hu, L. (2017). A review of physics and correlations of pool fire behaviour in wind and future challenges. *Fire Safety J*. 91, 41–55. doi: 10.1016/j.firesaf.2017.05.008

Hu, L., Hu, J., and de Ris, J. (2015). Flame necking-in and instability characterization in small and medium pool fires with different lip heights. *Combust. Flame* 162, 1095–1103. doi: 10.1016/j.combustflame.2014.10.001

Imura, H., Gilpin, R. R., and Cheng, K. C. (1978). An experimental investigation of heat transfer and buoyancy induced transition from laminar forced convection to turbulent free convection over a horizontal isothermally heated plate. *J. Heat Transf*. 100, 429–434. doi: 10.1115/1.3450826

Johnson, M. R., and Kostiuk, L. W. (2000). Efficiencies of low-momentum jet diffusion flames in crosswinds. *Combust. Flame* 123, 189–200. doi: 10.1016/S0010-2180(00)00151-6

Miller, C., Tang, W., Finney, M., McAllister, S., Forthofer, J., and Gollner, M. (2017). An investigation of coherent structures in laminar boundary layer flames. *Combust. Flame* 181, 123–135. doi: 10.1016/j.combustflame.2017.03.007

Moorhouse, J. (1982). Scaling criteria for pool fires derived from large-scale experiments. *Intl. Chem. Sym*. 71, 165–179.

Putnam, A. A. (1965). A model study of wind-blown free-burning fires. *Proc. Comb. Inst.* 10, 1039–1046. doi: 10.1016/S0082-0784(65)80245-4

Quintiere, J. (1989). Scaling applications in fire research. *Fire Safety J.* 15, 3–29. doi: 10.1016/0379-7112(89)90045-3

Subbarao, E. R., and Cantwell, B. J. (1992). Investigation of a co-flowing buoyant jet: experiments on the effect of Reynolds number and Richardson number. *J. Fluid Mech.* 245, 69–90. doi: 10.1017/S0022112092000351

Tang, W., Gorham, D., Finney, M., McAllister, S., Cohen, J., Forthofer, J., et al. (2017b). An experimental study on the intermittent extension of flames in wind-driven fires. *Fire Safety J.* 91, 742–748. doi: 10.1016/j.firesaf.2017.03.030

Tang, W., Miller, C., and Gollner, M. (2017a). Local flame attachment and heat fluxes in wind-driven line fires. *Proc. Combust. Inst.* 36, 3253–3261 doi: 10.1016/j.proci.2016.06.064

Thomas, P. H. (1963). The size of flames from natural fires. *Proc. Combust. Inst.* 9, 844–859. doi: 10.1016/S0082-0784(63)80091-0

Weckman, E. J., and Sobiesiak, A. (1988). The oscillatory behaviour of medium-scale pool fires. *Proc. Combust. Inst.* 22, 1299–1310. doi: 10.1016/S0082-0784(89)80141-9

Conflict of Interest Statement: The authors declare that the research was conducted in the absence of any commercial or financial relationships that could be construed as a potential conflict of interest.